

322
VLUV

SLL 81 417



DISTRIBUTION STATEMENT A

Approved for public release;
Distribution Unlimited

ON THE ROAD TO COMPUTATIONAL ACOUSTICS

by

H. Dwight Hogge

A Paper Presented at the 96th Meeting
of The Acoustical Society of America
Honolulu, Hawaii

27 November - 1 December 1978

19980309 377

DTIC QUALITY INSPECTED
PLEASE RETURN TO:

BMD TECHNICAL INFORMATION CENTER
BALLISTIC MISSILE DEFENSE ORGANIZATION
7100 DEFENSE PENTAGON
WASHINGTON D.C. 20301-7100

POSEIDON RESEARCH

11777 San Vicente Boulevard • Los Angeles, California 90047

U3809

Accession Number: 3809

Publication Date: Dec 01, 1978

Title: On the Road to Computational Acoustics, a Paper Presented at the 96th Meeting of the Acoustical Society of America, Honolulu, HA, 27 November - 1 December 1978

Personal Author: Hogge, H.D.

Corporate Author Or Publisher: Poseidon Research, 11777 San Vicente Boulevard, Los Angeles, CA 90049

Report Prepared for: Defense Advanced Research Projects Agency, 1400 Wilson Blvd., Arlington, VA 22209 Report Number
Assigned by Contract Monitor: SLL 81 417

Comments on Document: Archive, RRI, DEW.

Descriptors, Keywords: Directed Energy Weapon DEW Computational Acoustics Fluid Dynamics Numeric Integration Nonsteady Compressible Continuity Momentum Energy Equation Nonlinear Convection Viscosity SHASTA Piston Drive Shock Wave

Pages: 24

Cataloged Date: Oct 19, 1992

Document Type: HC

Number of Copies In Library: 000001

Record ID: 24991

Source of Document: DEW

**ON THE ROAD TO
COMPUTATIONAL ACOUSTICS**

by

H. Dwight Hogge

**A Paper Presented at the 96th Meeting
of The Acoustical Society of America
Honolulu, Hawaii**

27 November - 1 December 1978

**POSEIDON RESEARCH
11777 San Vicente Boulevard
Los Angeles, California 90049**

ON THE ROAD TO COMPUTATIONAL ACOUSTICS

H. Dwight Hogge, Research Scientist
Poseidon Research, Los Angeles, California

Abstract

Acousticians have largely overlooked the methods of *computational fluid dynamics* (i.e., the direct numerical integration of the nonsteady, compressible continuity, momentum, and energy equations) because of the success of the linearized normal-mode approach and because the numerical viscosity inherent in traditional computational methods damps out acoustic disturbances at an unrealistic rate. The advantage of the computational approach is that it allows inclusion of physical phenomena excluded from the linearized normal-mode approach such as nonlinear convection, non-isentropic losses, and phase change effects. The recent development of SHASTA, a relatively nondiffusive computational method [J. P. Boris and D. L. Book, J. Comp. Physics 11, 38-69 (1973)], has made possible the accurate solutions to acoustics problems. SHASTA is applied to a piston driven shock wave, an acoustic traveling wave, and an acoustic standing wave. The solutions of these problems by other standard numerical schemes are shown for comparison. It is found that only SHASTA is acceptable for all problems considered. As a practical example the computational approach is applied to the acoustic-wave/entropy-wave interaction associated with reflections from a choked flow wall.

1. Introduction

For centuries the science of acoustics has prospered on the tremendous successes achieved by the use of linear theory. An incredible number of physical phenomena can be quite adequately analysed and modeled by the use of such techniques as normal mode expansions and Green's functions. In fact, this method of analysis has become a major component of the field of classical mathematical physics. The small (but not unimportant) portions of the field of acoustics that cannot be adequately modeled by linear theory have been by far overshadowed by the successes of linear theory.

In recent decades, workers in the field of nonsteady gas-dynamics have developed methods of solving nonlinear problems by purely computational techniques. The thrust of the effort has been aimed at the difficult problem of numerical solutions to hyperbolic partial differential equations with discontinuous solutions--in other words, the mathematical theory of shock waves. The result has been a sophisticated technology finely tuned to give the best possible representation of shock waves. The most successful of such theories are those of Von Neumann and Richtmyer (1950), which is a Lagrangian approach, and Lax and Wendroff (1960), which is an Eulerian approach. These theories represent the state of the art as of twenty and ten years ago, respectively.

Although the classical computational methods of Von Neumann-Richtmyer and Lax-Wendroff were developed explicitly for the solution of shock wave problems, it is possible to apply them to linear acoustics problems. As will be shown in this paper, the solution to linear problems using these methods can be satisfactory under certain circumstances. On many occasions, however, it is necessary to supplement the numerical diffusion of the classical methods with a linear artificial viscosity

in order to stabilize the solution. On those occasions, the linear damping makes solution to linear acoustics problems impossible. The classical methods represent an essentially nonresolvable conflict between stability and nondiffusiveness.

More recently a new method called SHASTA was developed by Boris and Book (1973). This method has the particular advantage that it provides the numerical stability required to solve shock wave problems yet retains the degree of nondiffusivity required to solve linear problems. The main objective of this paper is to demonstrate the problems associated with the classical methods and to show that SHASTA overcomes these problems.

2. The Governing Equations

Computational acoustics, like its parent computational fluid dynamics, is simply the direct numerical solution of the primitive conservation equations of gas dynamics--namely, for one-dimensional flows, the conservation of mass:

$$\frac{\partial \rho}{\partial t} + \frac{\partial}{\partial x}(\rho u) = 0 , \quad (1)$$

the conservation of momentum:

$$\frac{\partial}{\partial t}(\rho u) + \frac{\partial}{\partial x}(\rho u^2) = - \frac{\partial}{\partial x}(P + Q) , \quad (2)$$

and the conservation of energy:

$$\frac{\partial}{\partial t}(\rho e) + \frac{\partial}{\partial x}(\rho u e) = - (P + Q) \frac{\partial u}{\partial x} . \quad (3)$$

The set of equations is closed by the equations of state:

$$P = (\gamma - 1)\rho e , \quad (4)$$

and

$$Q = \begin{cases} C_o^2 \rho (\Delta u)^2 - C_1 \rho c \Delta u , & \Delta u < 0 \\ 0 & \Delta u \geq 0 . \end{cases} \quad (5)$$

The parameters involved in (1) through (5) are as follows:

ρ = density

u = velocity

P = pressure
 Q = artificial viscosity stress
 e = internal energy per unit mass
 γ = ratio of specific heats
 c = local speed of sound
 C_0^2 = quadratic artificial viscosity coefficient
 C_1 = linear artificial viscosity coefficient.

Note these are the inviscid equations of gas dynamics altered by the addition of an artificial viscosity term represented by the stress Q . This extra pressure-like term is added because it was necessary to stabilize the solution by the classical methods of Von Neumann-Richtmyer or Lax-Wendroff. For those methods it is typical to set $C_0^2 = 0.5$ and $C_1 = 1$. As will be shown in the next section, Lax-Wendroff can provide solutions to linear problems with $C_1 = 0$. Furthermore, note that the SHASTA does not require artificial viscosity to stabilize the solution and hence for SHASTA calculations set $C_0^2 = C_1 = 0$.

In the following section we will present solutions to some simple example problems by the Lax-Wendroff method and the SHASTA method. The difference between the two methods is the way in which the advective term is handled. To illustrate the point and define the algorithms used, let us consider only the continuity equation (1). If the value of density at time $t_n = n\Delta t$ and spatial point $x_j = j\Delta x$ is given by ρ_j^n , then the value at the next time step $t_{n+1} = (n+1)\Delta t$ is given by ρ_j^{n+1} . Lax-Wendroff (specifically the so-called two-step Lax-Wendroff) is a two step process given by

$$\rho_j^{n+1} = \rho_j^n - \left[\rho_{j+1/2}^{n+1/2} \epsilon_{j+1/2}^{n+1/2} - \rho_{j-1/2}^{n+1/2} \epsilon_{j-1/2}^{n+1/2} \right], \quad (6)$$

where

$$\rho_{j+1/2}^{n+1/2} = \frac{1}{2}[\rho_{j+1}^n + \rho_j^n] - \frac{1}{2}[\rho_{j+1}^n \epsilon_{j+1}^n - \rho_j^n \epsilon_j^n], \quad (7)$$

and where

$$\epsilon_j^n = u_j^n \Delta t / \Delta x. \quad (8)$$

The SHASTA algorithm is more complicated and will not be repeated here. The actual equations used in the calculations to be given here are exactly as in the paper by Boris and Book. It should be noted that SHASTA is a hybrid scheme not derivable from a Taylor series expansion of the spatial derivatives. Hence it is not possible to give exactly the order of accuracy. It is claimed, however, that SHASTA (like Lax-Wendroff) is second-order accurate in regions where the solution is smooth. SHASTA is a two step method--the first step being a transport step with large diffusion, which provides stability. The second step is an anti-diffusion step wherein most of the diffusion added by the transport step is removed. As a result the final answer is stable and relatively nondiffusive.

3. Some Simple Examples

In this section, the application of SHASTA and Lax-Wendroff to several simple examples is given. The problems solved are: (1) a Mach 3 shock wave, (2) a 100 dB traveling wave, and (3) a 100 dB standing wave. The objective of this study is to demonstrate the dynamic range capable of SHASTA. The Mach 3 shock wave represents a pressure disturbance of about ten atmospheres. The 100 dB linear waves represent pressure disturbances of about 2×10^{-5} atmospheres. Hence the total range covered in these examples is six orders of magnitude.

Figures 1 and 2 are the results of solving the Mach 3 shock wave problem. The solid lines are the exact solution and the symbols are the numerical calculation. The solid line on the left-hand-side of each figure is the initial shock wave shape. The solid line on the right-hand-side of each figure is the exact shock wave shape at the time corresponding to the numerical solution. The total duration of the calculation is the time required for the Mach 3 wave to propagate the distance occupied by 100 computational cells. Comparison of the two methods shows that the main difference is the amount of spreading of the discontinuity. Some spreading is inherent to any finite-difference solution but should be kept to a minimum. The SHASTA solution has produced a shock front occupying about 3 cells. The Lax-Wendroff solution, on the other hand, has the shock front occupying about 8 cells. It should be noted that this difference in the amount of spreading of the shock front could be very important from an acoustics point of view because it represents a loss of high frequency content of the wave.

Figures 3 and 4 are the results of solving the 100 dB traveling wave problem. As before, the solid line is the exact solution and the symbols are the numerical solution. The data shown is the pressure

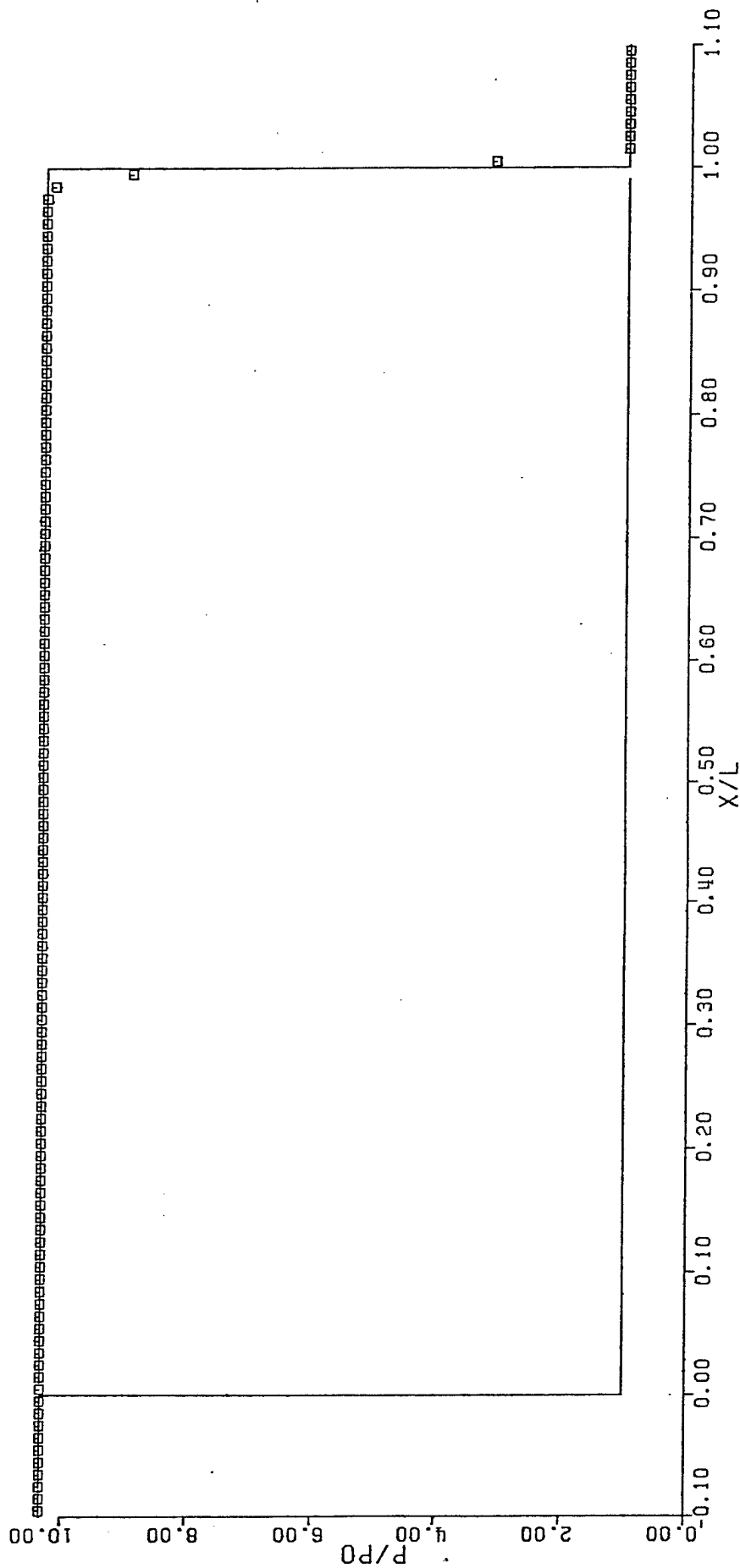


Figure 1. Mach 3 shock wave problem as solved by SHASTA method.

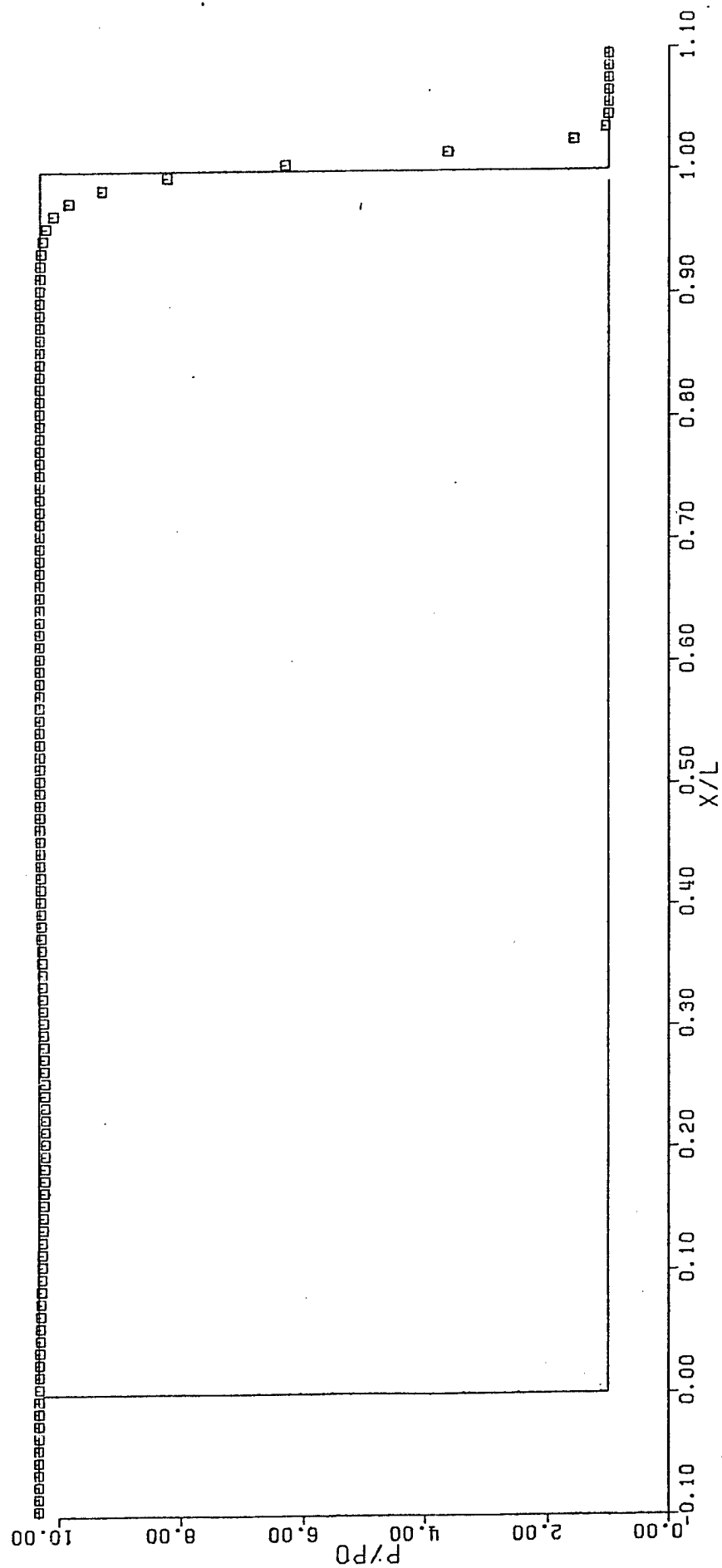


Figure 2. Mach 3 shock wave problem as solved by Lax-Wendroff method.

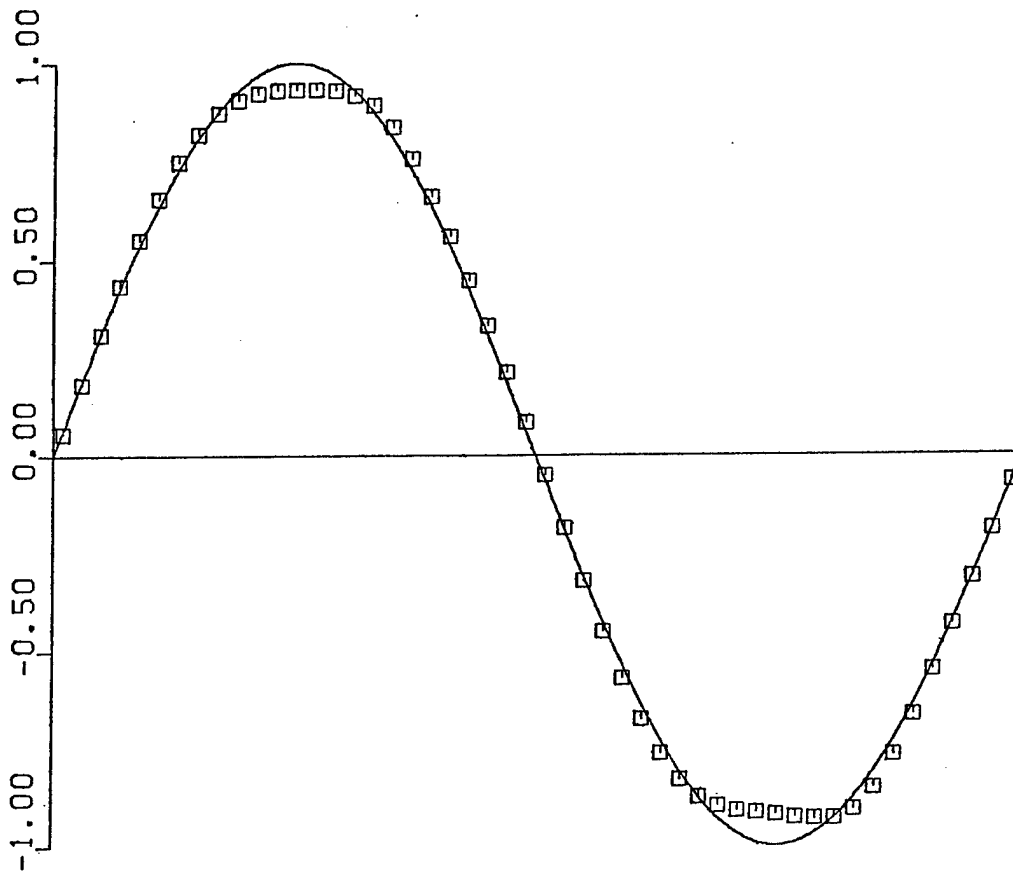


Figure 3. 100 dB traveling wave problem as solved by SHASTA method.

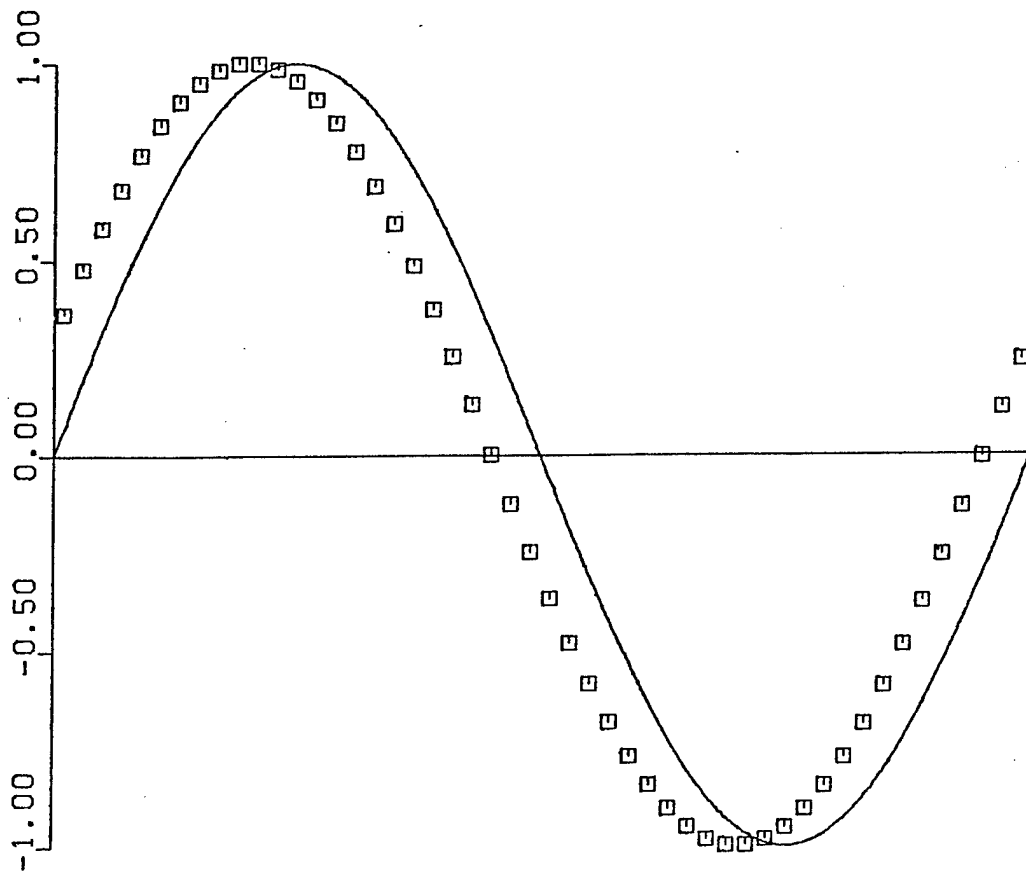


Figure 4. 100 dB traveling wave problem as solved by Lax-Wendroff method with $C_1 = 0$.

wave form after the wave has traveled 20 wavelengths. The resolution is 50 computational cells per wavelength. The result is that the SHASTA solution follows the wave very well except for a slight clipping of the wave peaks. This clipping phenomena has been seen in other calculations and seems to be characteristic of the method (see Boris and Book for further discussion). The Lax-Wendroff solution retains the wave shape and amplitude very well but has a slight phase shift. This phase shift should not be considered extremely important, however, since it is a small fraction of a wavelength after a total propagation length of 20 wavelengths.

Figures 5 and 6 are the results of solving the 100 dB standing wave problem. Again, the solid line is the exact solution and the symbols are the numerical calculations. The data shown is the pressure wave form after the wave has oscillated 20 periods. As before, the resolution is 50 cells per wavelength. The result is that both SHASTA and Lax-Wendroff do an excellent job on this problem. Each shows only a slight amount of damping with the Lax-Wendroff somewhat more damped than the SHASTA solution. It should be noted that all of the Lax-Wendroff calculations shown thus far have been with the linear artificial damping turned off (i.e., $C_1 = 0$). It is not always possible to run in that mode, however. It has been observed in the past that Lax-Wendroff, and in fact any of the earlier methods such as the Von Neumann-Richtmyer Lagrangian technique, can produce high frequency ripples. The standard method of controlling the ripples is to use the linear artificial viscosity with $C_1 = 1$. As shown in figure 7, that procedure completely damps out the linear wave. It is essential that linear artificial viscosity not be used if small level linear phenomena are being calculated. The SHASTA, of course, does not use either term of the artificial viscosity (i.e., $Q = 0$) and so does not suffer from the linear damping shown in figure 7.

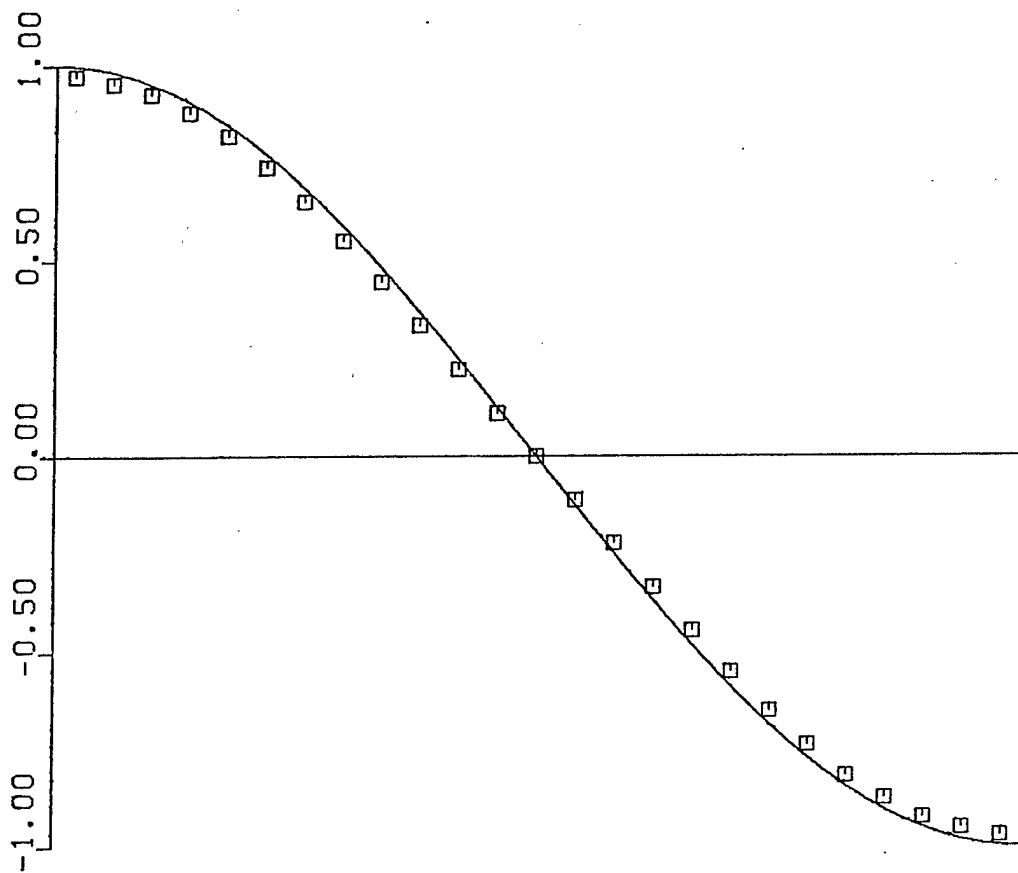


Figure 5. 100 dB standing wave problem as solved by SHASTA method.

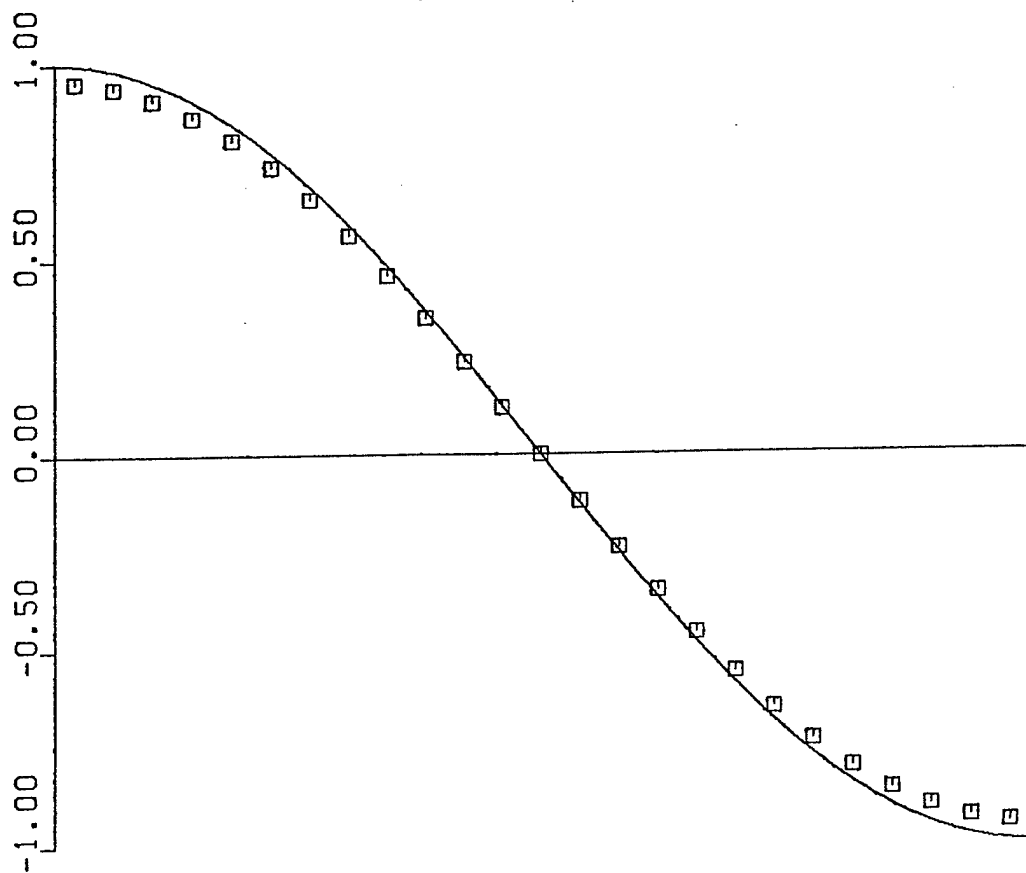


Figure 6. 100 dB standing wave problem as solved by Lax-Wendroff method with $C_1 = 0$.

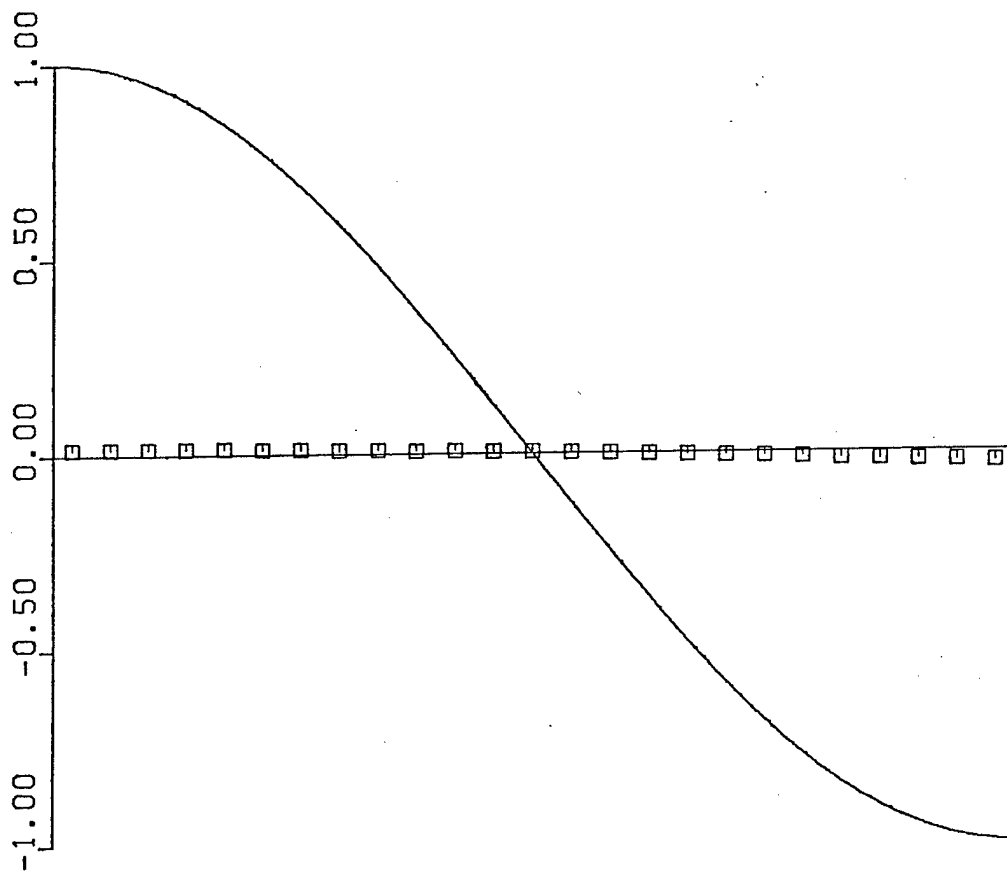


Figure 7. 100 dB standing wave problem as solved by Lax-Wendroff method with $C_1 = 1$.

In summary, SHASTA works fine for both large disturbance and linear problems of the type considered here. Lax-Wendroff also works, but not as well, for the large disturbance problem and for the linear problem provided the linear artificial viscosity is not used.

4. A Practical Example - Acoustic-Wave/Entropy-Wave Interaction Associated with Reflections from a Choked Flow Wall

In the preceding section, we demonstrated the ability of a SHASTA computational acoustics code to solve several simple example problems for which the exact solution is known. In this section we show the solution to a somewhat more interesting problem with practical application. The problem considered here is the reflection of an acoustic wave from a choked flow wall. The problem is of interest because choked flow walls are used as a means of isolating the fluid in the plenum upstream of the wall from disturbances that occur downstream. This is commonly done in pulsed high power lasers where the gas flowing into the active region is intermittently disturbed by a laser pulse and yet must be cleared of disturbances between pulses.

Physically, a choked flow wall is simply a plate normal to the flow direction with holes for the gas to flow through. The holes are small enough and the pressure ratio across the wall is large enough so that the flow through the holes is choked. The jets exiting the holes are underexpanded supersonic jets that go through a mixing process downstream of the flow wall before they combine into a uniform flow. Figure 8 is a schematic of the flow downstream of a single flow wall hole. The essential fluid dynamic features of the flow process are that the stagnation enthalpy and mass flow are fixed by the plenum conditions and that the temperature and density of the fluid downstream of the jets are set by the applied pressure. This thermodynamic connection is nonisentropic so that pressure waves which reflect off the flow wall generate entropy waves as well as the usual reflected pressure waves. The entropy waves are isobaric temperature and density disturbances that convect with the flow.

The results of the computational study of this process are given in figures 9 and 10. Figure 9 is pressure data and figure 10 is density

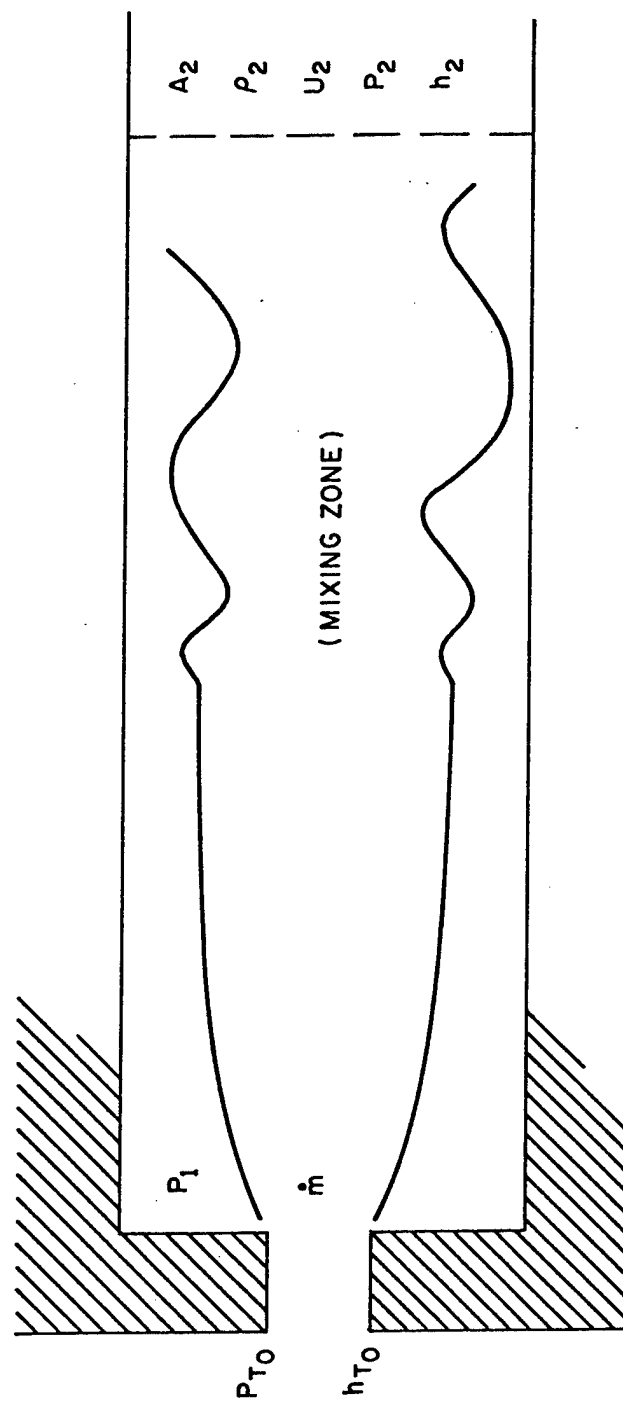
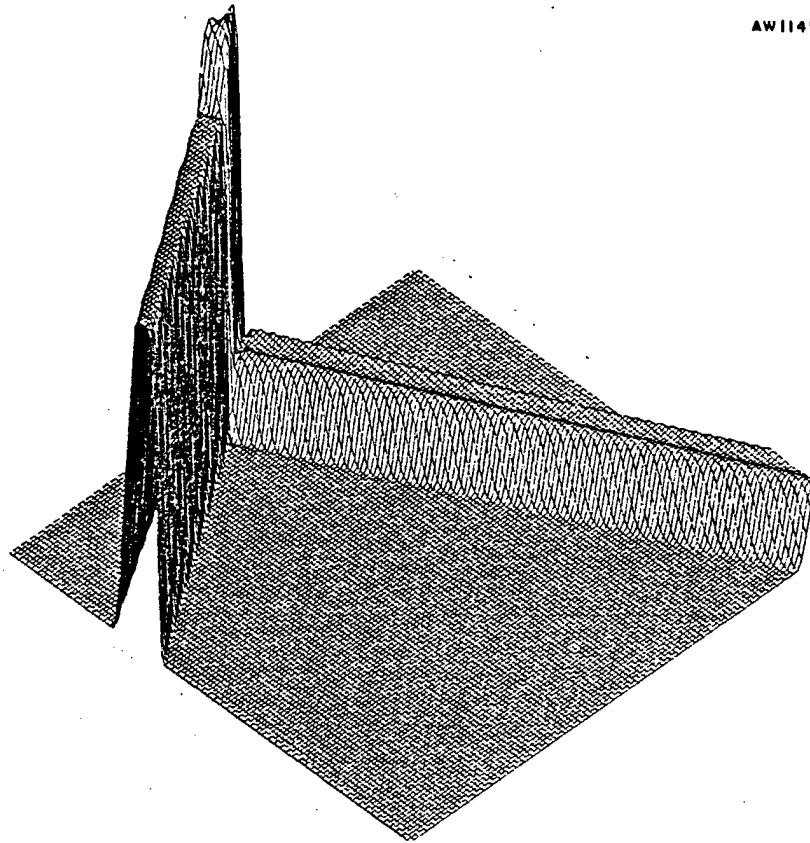


Figure 8. Schematic of choked flow wall configuration.



$$\Delta P/P_0 = 0.01$$

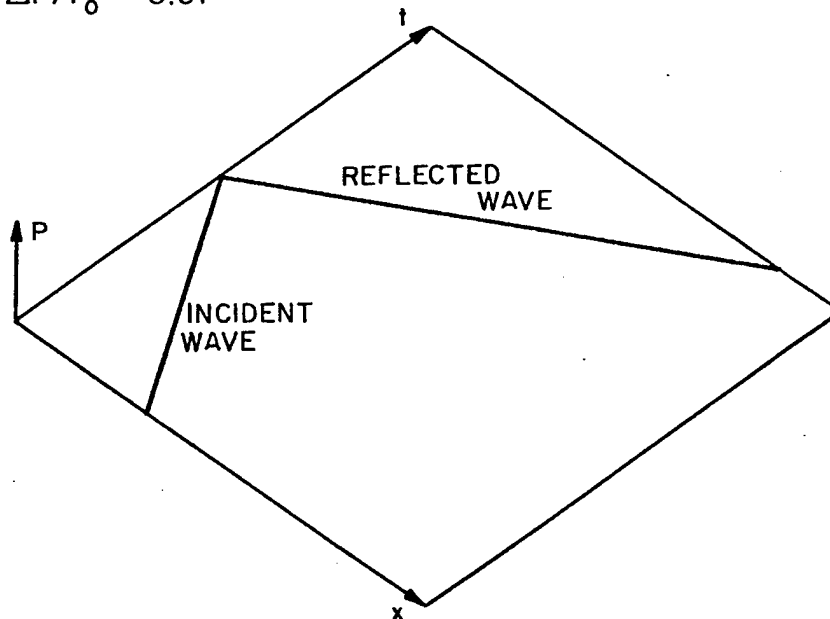


Figure 9a. Pressure in x-t space resulting from choked flow wall reflection problem.

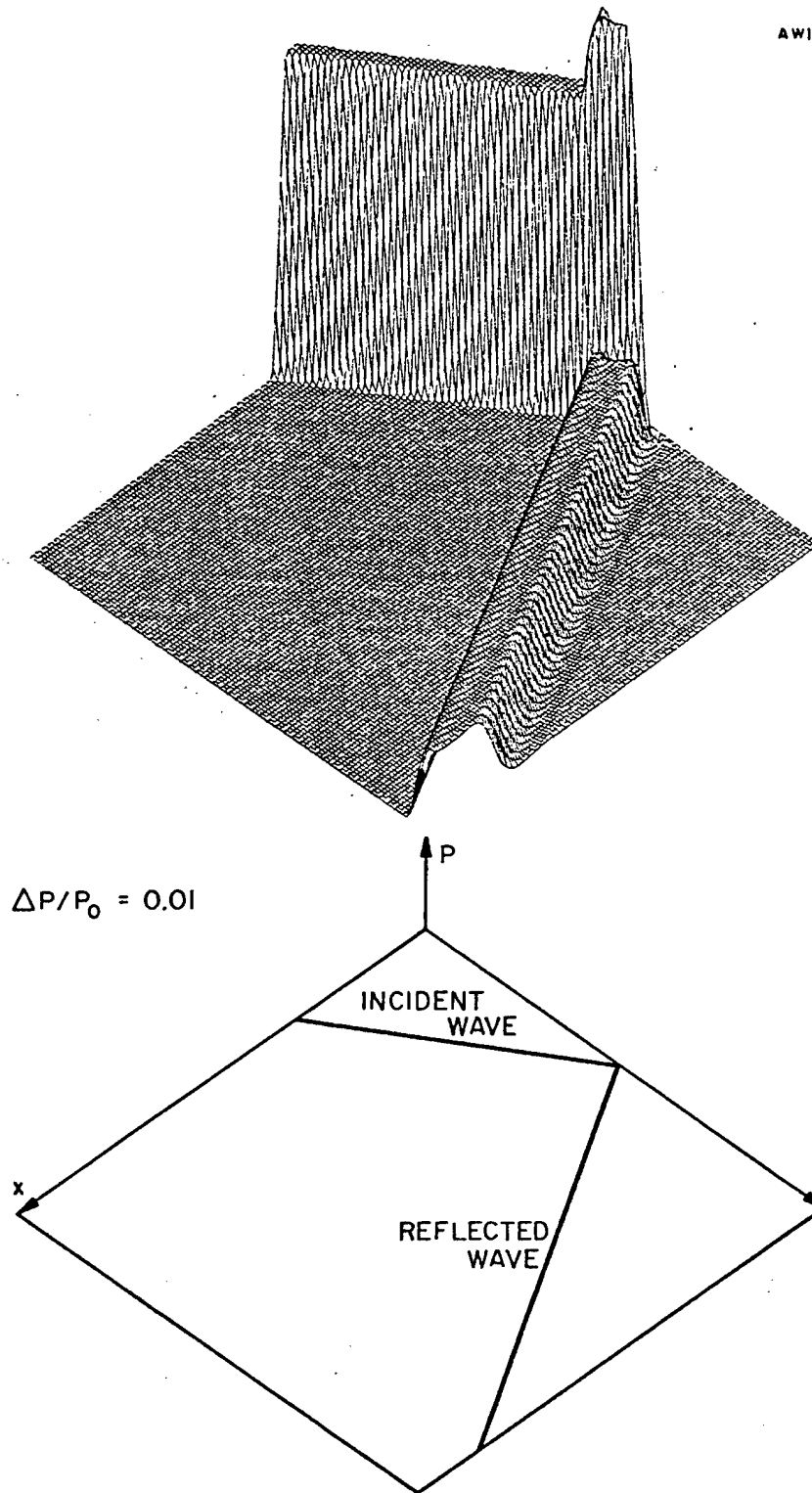
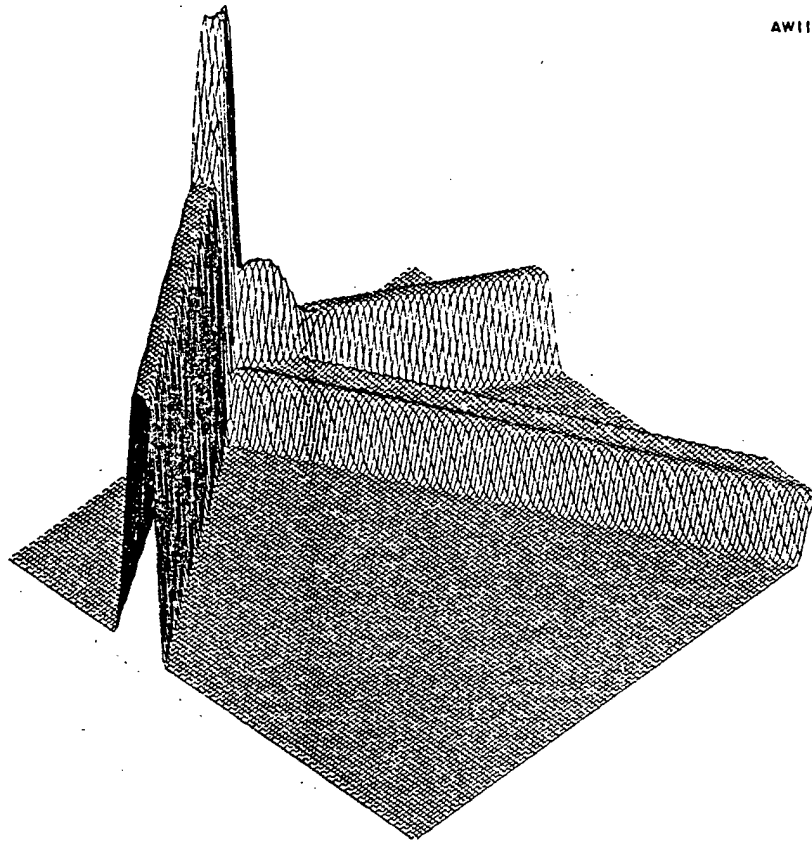


Figure 9b. Same data as shown in figure 9a but from a different angle.



$$\Delta P/P_0 = 0.01$$

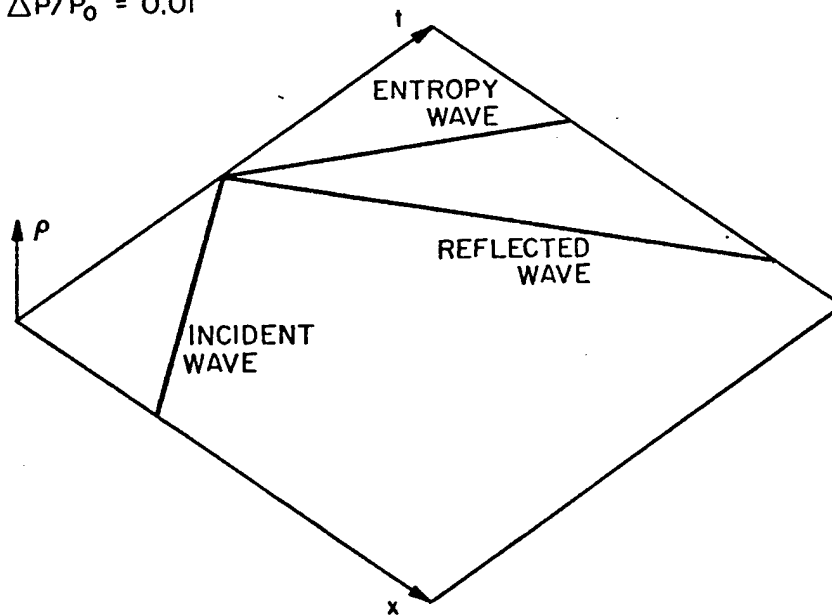


Figure 10a. Density in x-t space resulting from choked flow wall reflection problem showing entropy wave.

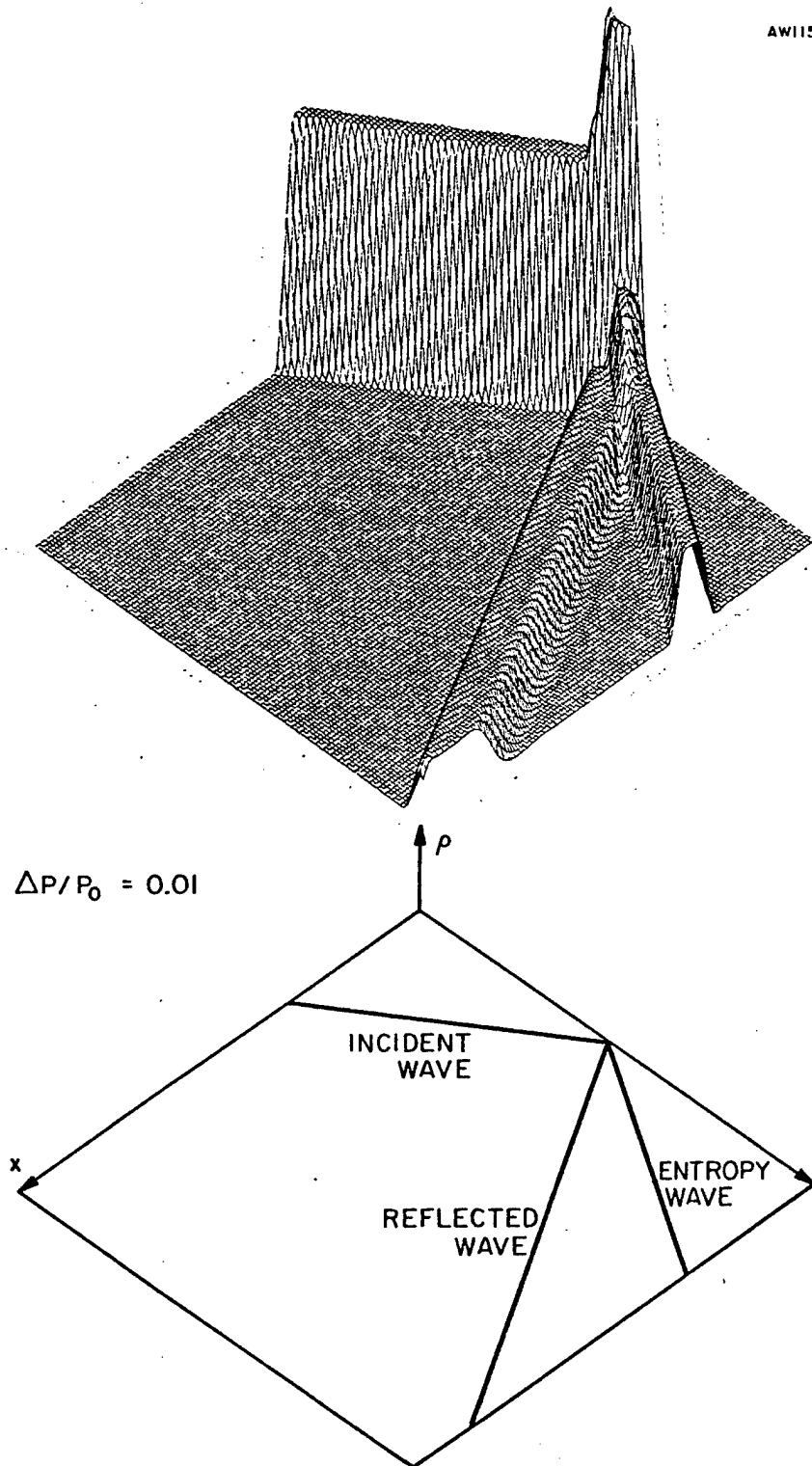


Figure 10b. Same data as shown in figure 10a but from a different angle.

data. Each figure is a three-dimensional plot of the dependent variable in x - t space superimposed on an x - t diagram with the characteristics of the disturbances indicated. Also each figure consists of an a and b part, which are different only in the angular orientation of the plot. The initial condition is a trapezoidal pressure pulse situated downstream of the flow wall and propagating upstream. The flow wall is located at the origin of the x -coordinate. As seen in figure 9, the pressure pulse propagates upstream, hits the flow wall and reflects downstream. The entropy wave does not show on figure 9 because it is an isobaric disturbance.

Figure 10 shows the density disturbance in x - t space. Each of the pressure waves identified in figure 9 has a corresponding density disturbance (the pressure waves are isentropic). In addition, figure 10 shows the entropy wave produced by the reflection. The entropy wave is convecting with the flow, which in this case is a Mach 0.5 flow.

The reflection of pressure waves from choked flow walls can be treated in analytical form in the limit of small disturbances. This linear analysis is given by Hogge (1978) and is in agreement with the results given here as it should be since the disturbance level here is 0.01 atmospheres.

5. Conclusions

It has been shown that computational acoustics was only marginally possible using earlier methods because of the conflict between numerical stability and numerical diffusion. The SHASTA method, on the other hand, overcomes that difficulty and makes it possible to do both large disturbance shock wave problems and linear acoustics problems. The method of computational acoustics makes it possible to do many problems that cannot be successfully done by the linear normal mode approach such as nonlinear waves, problems with bulk absorption and heat transfer, and problems with chemical reactions and phase change. In fact, the method has already been used effectively in several previous research programs (Hogge and Crow 1977, 1978a, and 1978b).

Acknowledgment

This work was supported by the Defence Advanced Research Projects Agency and the Naval Research Laboratory with Dr. S. K. Searles as the technical monitor.

References

1. Von Neumann, J. and Richtmyer, R. D. 1950 A method for the numerical calculation of hydrodynamic shocks. *Journal of Applied Physics* 21, 232-237.
2. Lax, P. and Wendroff, B. 1960 Systems of conservation laws. *Communications on Pure and Applied Mathematics* 13, 217-237.
3. Boris, J. P. and Book, D. L. 1973 Flux-corrected transport - Part I: SHASTA, a fluid transport algorithm that works. *Journal of Computational Physics* 11, 38-69.
4. Hogge, H. D. 1978a Interaction of entropy waves and acoustic waves in pulsed lasers. Poseidon Research Note No. 42, August.
5. Hogge, H. D. and Crow, S. C. 1977 Gasdynamics of pulsed chemical lasers. Poseidon Research Report No. 8, September.
6. Hogge, H. D. and Crow, S. C. 1978a Flow design concepts for high-power pulsed visible-wavelength lasers. Poseidon Research Report No. 16, May.
7. Hogge, H. D. and Crow, S. C. 1978b Flow and acoustics in pulsed excimer lasers. Presented at the AIAA Conference on Fluid Dynamics of High Power Lasers, October 31-November 2, 1978, Cambridge, Massachusetts.